Evidence of concentration fluctuations in disordered network-forming systems: the case of $GeSe_4$ and $SiSe_2$

2003 J. Phys.: Condens. Matter 15 S1537

(http://iopscience.iop.org/0953-8984/15/16/303)

INSTITUTE OF PHYSICS PUBLISHING JOURNAL OF PHYSICS: CONDENSED MATTER

J. Phys.: Condens. Matter **15** (2003) S1537–S1546 PII: S0953-8984(03)54810-X

Evidence of concentration fluctuations in disordered network-forming systems: the case of $GeSe_4$ and $SiSe_2$

Carlo Massobrio[1], **Massimo Celino**[2,3] **and Alfredo Pasquarello**[4,5]

[1] Institut de Physique et de Chimie des Matériaux de Strasbourg, 23 rue du Loess, F-67037 Strasbourg, France
[2] Ente per le Nuove Tecnologie, l'Energia e l'Ambiente, C R Casaccia, CP 2400, I-00100 Roma, Italy
[3] Istituto Nazionale per la Fisica della Materia, Unità di Ricerca Roma1, Italy
[4] Institut de Théorie des Phénomènes Physiques (ITP), Ecole Polytechnique Fédérale de Lausanne (EPFL), CH-1015 Lausanne, Switzerland
[5] Institut Romand de Recherche Numérique en Physique des Matériaux (IRRMA), CH-1015 Lausanne, Switzerland

Received 16 October 2002
Published 14 April 2003
Online at stacks.iop.org/JPhysCM/15/S1537

Abstract

In a search for the physical origin of the first sharp diffraction peak (FSDP) in the concentration–concentration partial structure factor $S_{CC}(k)$ of disordered network-forming materials, we perform first-principles molecular dynamics simulations of liquid $GeSe_4$ (l-$GeSe_4$) and liquid $SiSe_2$ (l-$SiSe_2$). These systems are designed to provide clues on the relationship between the appearance of an FSDP in the $S_{CC}(k)$ structure factor and the degree of chemical order. Short-range chemical order is more pronounced in l-$GeSe_4$ and in l-$SiSe_2$ than in liquid $GeSe_2$. For the latter system, our level of theory does not reproduce the FSDP in the experimentally observed $S_{CC}(k)$ structure factor. We find that a distinct FSDP shows up in the partial structure factor $S_{CC}(k)$ for l-$GeSe_4$. In $S_{CC}(k)$ for l-$SiSe_2$, we also find a feature at the FSDP location, although it is smaller compared to $GeSe_4$. Given the tight correlation existing between chemical order and ionicity, these results suggest that the ionic character of the bonds plays a crucial role in inducing concentration fluctuations at intermediate-range distances.

1. Introduction

The notion of intermediate-range order (IRO) refers to an enhanced level of structural organization involving distances well beyond nearest-neighbour interactions. While short-range order can be found in many liquids and glasses regardless of their stoichiometry or composition, IRO occurs mostly in disordered network-forming materials characterized by iono-covalent directional bonding [1]. IRO manifests itself through the appearance of a first sharp diffraction peak (FSDP) in the total neutron structure factor. This feature lies at a value

of the momentum transfer k close to half the momentum transfer of the principal diffraction peak [2]. In recent years, advances in the method of isotopic substitution in neutron diffraction have provided accurate partial structure factors, which provide detailed information on the contribution of the different correlations to the occurrence of the FSDP [1, 3]. The case of liquid $GeSe_2$ (l-$GeSe_2$) is particularly revealing. In this liquid, the appearance of an FSDP in the Bhatia–Thornton (BT) [4] concentration–concentration structure factor $S_{CC}(k)$ indicates fluctuations of concentration on distances typical of the IRO [3]. To appreciate the significance of the structure factor $S_{CC}(k)$ for a binary system made of A and X species it is convenient to look at its definition in terms of Faber–Ziman (FZ) [5] partial structure factors $S_{AA}(k)$, $S_{AX}(k)$ and $S_{XX}(k)$

$$S_{CC}(k) = c_A c_X[1 + c_A c_X((S_{AA}(k) - S_{AX}(k)) + (S_{XX}(k) - S_{AX}(k)))]. \quad (1)$$

We note that a peak at a given wavevector in $S_{CC}(k)$ stems from the sensitivity of a given atom (A or X) to the chemical nature of its neighbours, on the length scale associated with that specific value of k. In contrast, the absence of a peak corresponds to an equivalent tendency to homo-or heteropolar neighbours, favouring chemical disorder. For these reasons, $S_{CC}(k)$ is well suited to provide information on the length scales associated with spatial fluctuations around the average composition of the system.

To ascertain the microscopic structure of l-$GeSe_2$, first-principles molecular dynamics simulations based on density functional theory have been performed by using two different energy functionals, which reproduced differently the ionic character in the bonds [6–8]. The first functional we considered was a generalized gradient approximation (GGA) [9], while the second one was the local density approximation (LDA) [10]. Only the functional favouring more ionic bonding (GGA) gave rise to an FSDP in the calculated total neutron structure factor, in excellent agreement with experiment. The increase in the degree of ionicity was found to be correlated with an increase of short-range chemical order. In l-$GeSe_2$, the predominant structural unit is the $GeSe_4$ tetrahedron [7], coexisting with a non-negligible number of miscoordinated atoms and homopolar bonds.

Despite the appearance of an FSDP in the calculated total neutron structure factor, the results did not show an FSDP in the $S_{CC}(k)$ structure factor [6, 8]. In a subsequent set of simulations a further increase of ionicity in the treatment of the electronic structure was achieved through the use of a higher-energy cut-off in the expansion of the plane-wave basis set [11]. This choice led to a slightly better agreement with the experimental partial structure factors, a very small FSDP becoming discernable in the $S_{CC}(k)$ structure factor. Understanding the origins of the severe underestimate of this peak is a challenging step toward an improved theoretical description of IRO in liquids and glasses. Toward this goal, the sensitivity of chemical order to the ionic character of the bonding and its impact on the establishment of IRO provides guidance for further studies.

In this work we calculated the FZ and BT partial structure factors of liquid $GeSe_4$ (l-$GeSe_4$) and liquid $SiSe_2$ (l-$SiSe_2$) by first-principles molecular dynamics. Our aim is to establish whether an FSDP occurs in the partial structure factor $S_{CC}(k)$ of liquids exhibiting IRO but differing from l-$GeSe_2$ by a higher degree of short-range chemical order. In the case of l-$GeSe_4$, previous calculations were found to reproduce accurately the total neutron structure factor, showing that l-$GeSe_4$ is a good prototype of a chemically ordered network (CON) [12]. Therefore, it appears that a moderate increase in the Se/Ge ratio within the liquid $Ge_xSe_{(1-x)}$ family has a marked effect on chemical order. The study of l-$SiSe_2$ was recently undertaken as a prerequisite to the production of a suitable model of the amorphous phase, for which experimental data are available [13]. It was concluded that despite the same nominal value of the electronegativity of Ge and Si (1.8), short-range chemical order is higher in l-$SiSe_2$ than

in l-$GeSe_2$. This leads to a larger percentage of tetrahedra and a smaller number of homopolar bonds [14].

This paper is organized as follows. In section 2 we describe our theoretical model. Section 3 contains a brief description of the structural properties of l-$GeSe_2$, l-$GeSe_4$ and l-$SiSe_2$. The FZ structure factors and the BT concentration–concentration structure factors of l-$GeSe_2$, l-$GeSe_4$ and l-$SiSe_2$ are shown and analysed in section 4. Concluding remarks are collected in section 5.

2. Theoretical model

Our simulations were performed at constant volume. For l-$GeSe_4$ the system consists of $N = 120$ atoms (24 Ge and 96 Se). Two sizes were used for l-$SiSe_2$, with $N = 120$ (40 Si and 80 Se) and $N = 144$ (48 Si and 96 Se) atoms. We used periodically repeated cubic cells of size 16 Å (l-$GeSe_4$), 15.61 Å (l-$SiSe_2$, $N = 120$) and 16.56 Å (l-$SiSe_2$, $N = 144$). These values correspond to the experimental density of the liquid at $T = 1073$ K for l-$GeSe_4$ [15] and to the experimental density of amorphous $SiSe_2$ at $T = 300$ K for l-$SiSe_2$ [16]. The smallest wavevector compatible with our supercells is $k_{\min} \sim 0.4$ Å^{-1}. This wavevector is significantly smaller, for the three systems under consideration, than the FSDP wavevector $k_{\mathrm{FSDP}} \sim 1$ Å^{-1}.

The electronic structure was described within density functional theory (DFT) and evolved self-consistently during the motion [17]. In both calculations the GGA introduced by Perdew *et al* [9] was used for the treatment of the exchange and correlation energy. Valence electrons were taken into explicit account, in conjunction with norm-conserving pseudopotentials to describe core–valence interactions. The pseudopotentials were generated as in [18]. The wavefunctions were expanded at the Γ point of the supercell on a plane-wave basis set defined by energy cut-offs $E_c = 10$ and 20 Ryd for l-$GeSe_4$ and l-$SiSe_2$, respectively. Further details on the parameters of our simulations can be found in published work on the structure of l-$GeSe_4$ [12] and l-$SiSe_2$ [14].

In the case of l-$GeSe_4$ our starting configuration was the last produced in the study of [12]. We carried out a new set of simulations at $T = 1075$ K over a time period of 10 ps. We discarded the initial segment of 1 ps when taking statistical averages. The initial atomic positions for l-$SiSe_2$($N = 120$) were assigned randomly in the simulation box. Then the temperature was first raised to $T = 4000$ K and then gradually lowered to 1000 K during a time period of 15 ps. At $T = 1000$ K the system evolved for an additional 15 ps, with statistical averages calculated over the last 9 ps. The initial configuration for l-$SiSe_2$($N = 144$) was obtained by adapting the crystal structure of $SiSe_2$ to the cubic symmetry. This system was melted and thermalized at $T = 1000$ K for 15 ps, with statistical averages calculated over the last 5 ps. The results reported here are the mean values of the average properties over the two temporal evolutions with $N = 120$ and 144. No systematic size effect dependence of the results was found and, in particular, the location of the FSDP did not change from $N = 120$ to 144 in l-$SiSe_2$. The simulations were performed using the computer program described in [19] and [20] for norm-conserving pseudopotentials.

3. Structural properties

Analogies and differences among the topologies of l-$GeSe_4$, l-$SiSe_2$ and l-$GeSe_2$ are highlighted in table 1, where we give the nearest-neighbour coordination numbers n_α^β, where n_α^β is the average coordination number of an atom of species α by atoms of species β. The data in the table were extracted from previous structural studies on these systems [8, 12, 14]. In the

Table 1. Values for the coordination numbers n_{Ge}^{tot} and n_{Se}^{tot} and the total coordination number n^{tot} of l-$GeSe_2$, l-$GeSe_4$ and l-$SiSe_2$. For l-$GeSe_2$ and l-$GeSe_4$ the coordination numbers n_{Ge}^{tot} and n_{Se}^{tot} are given by $n_{\mathrm{Ge}}^{\mathrm{Ge}} + n_{\mathrm{Ge}}^{\mathrm{Se}}$ and $n_{\mathrm{Se}}^{\mathrm{Se}} + n_{\mathrm{Se}}^{\mathrm{Ge}}$, respectively. The total coordination number n^{tot} is equal to $c_{\mathrm{Ge}}(n_{\mathrm{Ge}}^{\mathrm{Ge}} + n_{\mathrm{Ge}}^{\mathrm{Se}}) + c_{\mathrm{Se}}(n_{\mathrm{Se}}^{\mathrm{Se}} + n_{\mathrm{Se}}^{\mathrm{Ge}})$, c_{Ge} and c_{Se} indicating the concentrations of Ge and Se atoms respectively. The same definitions hold for l-$SiSe_2$, with Si instead of Ge.

l-$GeSe_2$	$n_{\mathrm{Ge}}^{\mathrm{Ge}}$	$n_{\mathrm{Ge}}^{\mathrm{Se}}$	n_{Ge}^{tot}	$n_{\mathrm{Se}}^{\mathrm{Se}}$	$n_{\mathrm{Se}}^{\mathrm{Ge}}$	n_{Se}^{tot}	n^{tot}
Theory	0.04	3.76	3.80	0.37	1.88	2.25	2.77
RCN	2	2	4	1	1	2	2.67
CON	0	4	4	0	2	2	2.67
l-$GeSe_4$	$n_{\mathrm{Ge}}^{\mathrm{Ge}}$	$n_{\mathrm{Ge}}^{\mathrm{Se}}$	n_{Ge}^{tot}	$n_{\mathrm{Se}}^{\mathrm{Se}}$	$n_{\mathrm{Se}}^{\mathrm{Ge}}$	n_{Se}^{tot}	n^{tot}
Theory	0.06	3.87	3.93	1.04	0.97	2.01	2.39
RCN	1.33	2.67	4	1.33	0.67	2	2.4
CON	0	4	4	1	1	2	2.4
l-$SiSe_2$	$n_{\mathrm{Si}}^{\mathrm{Si}}$	$n_{\mathrm{Si}}^{\mathrm{Se}}$	n_{Si}^{tot}	$n_{\mathrm{Se}}^{\mathrm{Se}}$	$n_{\mathrm{Se}}^{\mathrm{Si}}$	n_{Se}^{tot}	n^{tot}
Theory	0.02	3.90	3.92	0.13	1.95	2.08	2.69
RCN	2	2	4	1	1	2	2.67
CON	0	4	4	0	2	2	2.67

case of l-$GeSe_4$, our new set of simulations reproduced the results of [12]. Table 1 also contains the n_α^β values for two models of network structure, the random covalent network (RCN) and the CON [21]. Both are compatible with the so-called $8-N$ rule, which gives the coordination number of an atom as a function of its column (N) in the periodic table. The structure of a liquid at a given composition follows the CON model when the number of heteropolar bonds is the largest possible for that composition. On the other hand, if there is no preference for either homopolar or heteropolar bonds, the RCN model holds. It is worth noticing that, for a given composition, the total coordination numbers for the CON model and the RCN model ($n_\alpha^{tot} = n_\alpha^\beta + n_\alpha^\alpha$) are the same. In the case of l-$GeSe_2$, the coordination numbers are $n_{\mathrm{Ge}}^{tot} = 3.80$ and $n_{\mathrm{Se}}^{tot} = 2.25$. The deviation from the $8 - N$ rule amounts to 12%. This liquid cannot be considered as chemically ordered since the $n_{\mathrm{Se}}^{\mathrm{Se}}$ coordination number differs noticeably from the CON value. Nevertheless, the CON model gives a much better approximation for the network structure of l-$GeSe_2$ than the RCN model. It is worthwhile recalling that the coordination numbers of l-$GeSe_2$ were found to be in good agreement with experimental estimates [7]. l-$GeSe_4$ and l-$SiSe_2$ are very close to a CON network. For l-$GeSe_4$ this means that the large majority of Ge atoms are in $GeSe_4$ tetrahedra, with some of the Se atoms necessarily forming homopolar bonds. Our data confirm that a transition from a network moderately departing from chemical order (l-$GeSe_2$) to a CON (l-$GeSe_4$) occurs for increasingly Se-rich compositions in Ge_xSe_{1-x} liquids.

4. Structure factors

In figure 1 we compare the total neutron structure factors $S_T(k)$ of l-$GeSe_2$, l-$GeSe_4$ and l-$SiSe_2$. The results for l-$GeSe_2$ are taken from [8]. The three $S_T(k)$ share a common pattern, in which the first three main peaks, lying at $k < 4$ Å^{-1}, are followed by less pronounced oscillations at higher k. The occurrence of IRO is clearly pointed out by a prominent FSDP found at about 1 Å^{-1}. In the case of l-$GeSe_4$ the present calculations reproduce the results of [12] for $k > 2$ Å^{-1} but the FSDP is distinctly higher and displaced to lower k values. The agreement with experiments for low k is worse than in the case of l-$GeSe_2$. Two reasons can

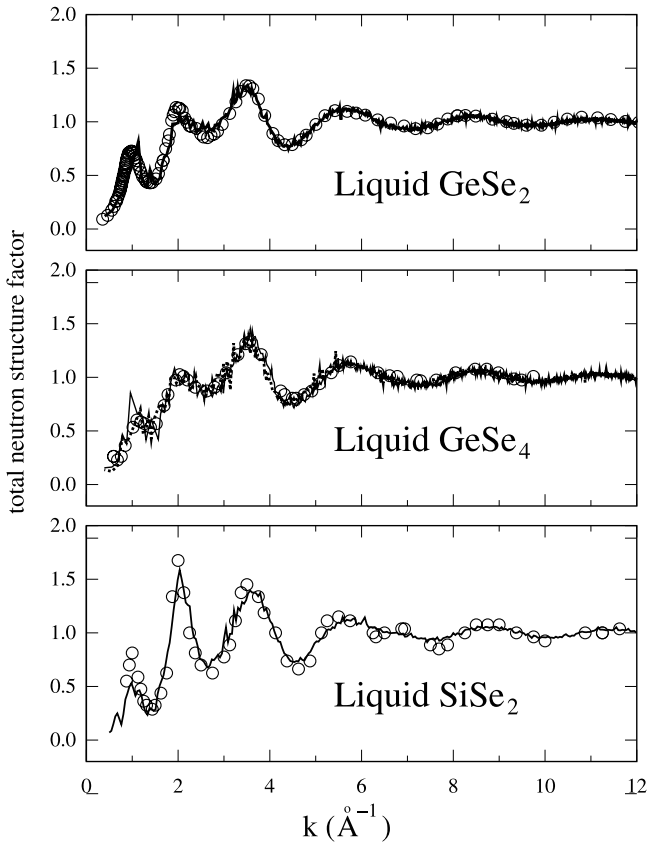

Figure 1. Top: calculated total neutron structure factor $S_T(k)$ of l-$GeSe_2$ compared to experimental data from [3] (circles). We used scattering lengths of $b_{Ge} = 8.189$ and $b_{Se} = 7.97$ fm. Middle: calculated total neutron structure factor $S_T(k)$ of l-$GeSe_4$ (solid curve, present results; dotted curve, results of [12]) compared to experimental data from [22] (circles). We used scattering lengths of $b_{Ge} = 8.189$ and $b_{Se} = 7.97$ fm. Bottom: calculated total neutron structure factor $S_T(k)$ of l-$SiSe_2$ (solid curve). The experimental results (circles) are the data for amorphous $SiSe_2$ from [16]. We used scattering lengths of $b_{Si} = 4.149$ and $b_{Se} = 7.97$ fm [16].

be invoked to account for this discrepancy. On the one hand, large fluctuations in the FSDP height are not unexpected. Typically, they are indicative of strongly time-dependent statistical averages on the timescale of our simulations [8]. On the other hand, the experimental data of figure 1 were obtained for a composition different from $x = 0.2$, the diffraction measurements being available for l-$Ge_{0.15}Se_{0.85}$ but not for l-$GeSe_4$ [22]. In [22], the FSDP was found to increase for increasing x values in the range 0–0.33, a maximum being attained at the l-$GeSe_2$ composition. Furthermore, the FSDP position moves to lower k for increasing x. These trends were recently confirmed by neutron diffraction measurements on Ge_xSe_{1-x} glasses [23]. The total neutron structure factor of l-$SiSe_2$ exhibits sharper maxima and minima. The FSDP height is lower than the experimental height for the $SiSe_2$ glass at the same density. This is consistent with the expected increase of the FSDP height for decreasing temperatures at constant density [24].

The calculated FZ partial structure factors of l-$GeSe_4$ and l-$GeSe_2$ are shown in figure 2. The partial structure factor $S_{GeGe}(k)$ of l-$GeSe_4$ shows a very prominent FSDP, and is more

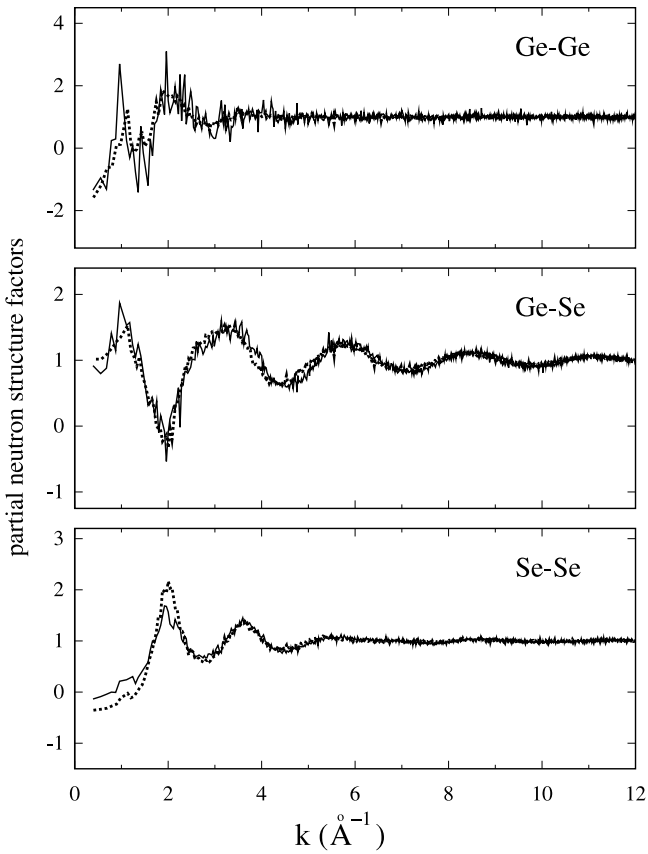

Figure 2. FZ partial structure factors for l-$GeSe_4$ (solid curve) and l-$GeSe_2$ (dotted curve). The results for l-$GeSe_2$ are taken from [8].

structured than the structure factor $S_{GeGe}(k)$ of l-$GeSe_2$. The latter is characterized by a smaller FSDP and a flatter first minimum. In l-$GeSe_4$ the Ge atoms belong almost exclusively to $GeSe_4$ tetrahedra, whereas a substantial number of Ge–Ge homopolar bonds were found in l-$GeSe_2$. It appears that the topology of l-$GeSe_4$ is correlated to a more enhanced ordering of Ge atoms on intermediate-range distances. The Ge–Se structure factors $S_{GeSe}(k)$ of l-$GeSe_4$ and l-$GeSe_2$ are quite similar over the entire k range, with a higher FSDP in l-$GeSe_4$. In the case of the structure factor $S_{SeSe}(k)$, the FSDP is essentially absent in both l-$GeSe_4$ and l-$GeSe_2$, but the main peak is lower and broader for l-$GeSe_4$. This feature can be associated with the presence in l-$GeSe_4$ of a larger number of Se chains, which accommodate the Se atoms not belonging to $GeSe_4$ tetrahedra.

In figure 3 the FZ partial structure factors of l-$SiSe_2$ are compared to those of l-$GeSe_2$. Overall the main peak, located at about 2 Å^{-1}, is higher and sharper in the l-$SiSe_2$ case, consistent with a larger number of Si-centred tetrahedra in this liquid. The FSDP stands out clearly in the $S_{SiSi}(k)$ and $S_{SiSe}(k)$ partial structure factors, while it is totally absent in $S_{SeSe}(k)$. The height of the FSDP in the partial structure factors $S_{SiSi}(k)$ and $S_{GeGe}(k)$ is comparable. Consequently, this implies that the intermediate-range correlations involving Si atoms in l-$SiSe_2$ are less important than those among Ge atoms in l-$GeSe_4$.

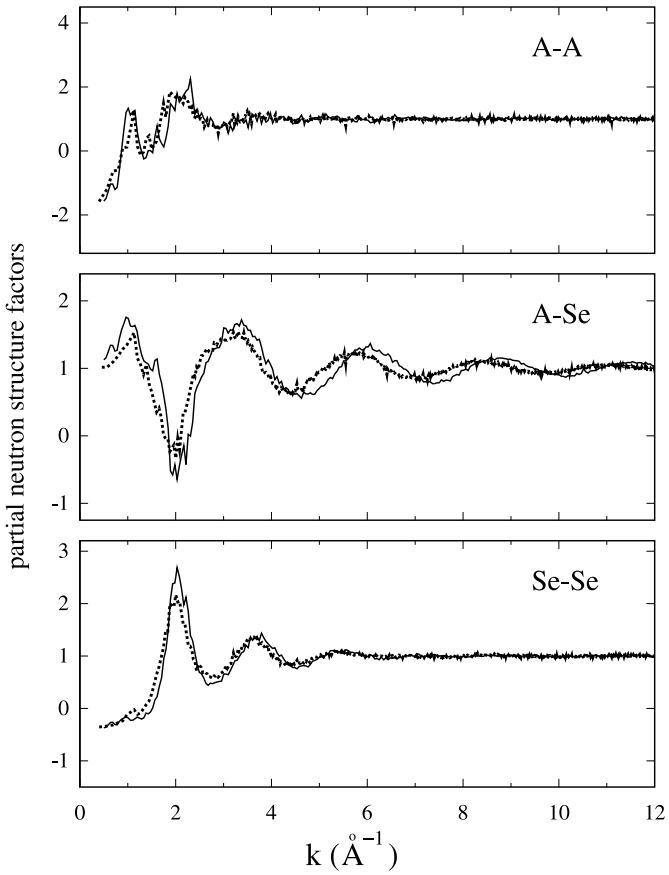

Figure 3. FZ partial structure factors for l-$SiSe_2$ (solid curve) and l-$GeSe_2$ (dotted curve). A stands for either Si or Ge. The results for l-$GeSe_2$ are taken from [8].

The calculated BT concentration–concentration partial structure factors $S_{CC}(k)$ of l-$GeSe_2$, l-$GeSe_4$ and l-$SiSe_2$ are presented in figure 4. Experimental results are only available for the case of l-$GeSe_2$ [3]. Our calculations do not reproduce the distinct feature at ~ 1 Å^{-1}. The simulation gives only a small peak in the FSDP region: the ratio between the heights of the first two peaks is equal to $0.12/0.43 = 0.28$, half the experimental value of 0.56. In l-$GeSe_4$ the large number of Se–Se bonds leads to a lowering of the main feature in the partial structure factor $S_{CC}(k)$ with respect to the l-$GeSe_2$ case. The identification of the marked signature at ~ 1 Å^{-1} with an FSDP is substantiated by the fact that the ratio between the heights of the first two peaks, i.e. 0.45, is much higher than for the calculated $S_{CC}(k)$ of l-$GeSe_2$. On the basis of the prominent FSDP in $S_{GeGe}(k)$ (figure 2) and by considering the expression for $S_{CC}(k)$ given in equation (1), one might infer that Ge–Ge correlations play a critical role in the appearance of an FSDP in the $S_{CC}(k)$ of l-$GeSe_4$. To corroborate this hypothesis, experimental data on the partial structure factors of l-$GeSe_4$ are highly desirable.

In the case of l-$SiSe_2$ a distinct bump is visible at the FSDP location in the partial structure factor $S_{CC}(k)$. We recall that l-$SiSe_2$ differs from l-$GeSe_2$ by a higher level of chemical order, i.e. by a larger number of fourfold-coordinated cations. The ratio between the heights of the first two peaks is close to the corresponding value in l-$GeSe_2$ (0.22 for l-$SiSe_2$ versus 0.28 for

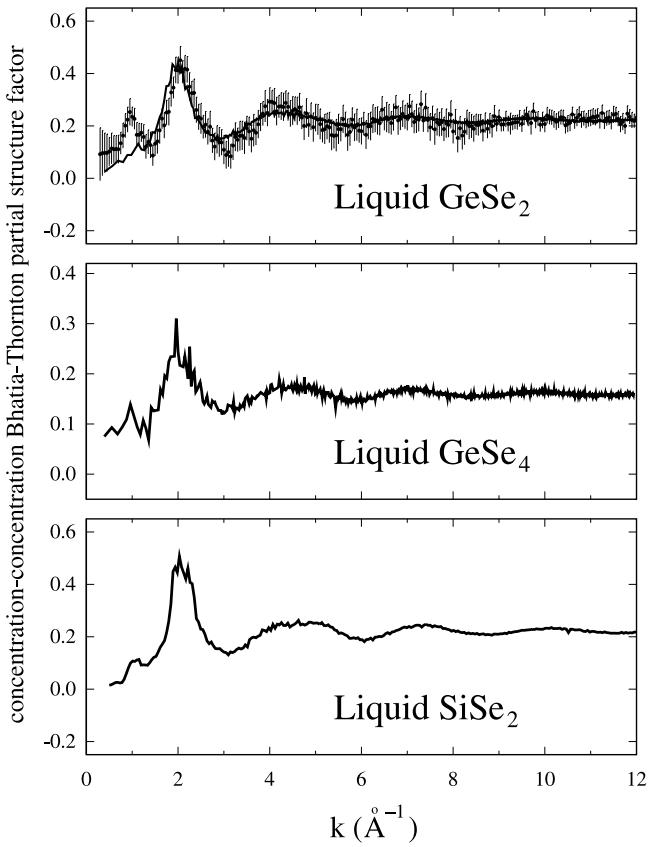

Figure 4. BT concentration–concentration partial structure factor $S_{CC}(k)$ for l-$GeSe_2$ [8], l-$GeSe_4$ and l-$SiSe_2$. The experimental data for l-$GeSe_2$ are those of [3].

l-$GeSe_2$). However, since the FSDP peak in $S_{CC}(k)$ appears to be more distinct, fluctuations of concentration are likely to be more important than in l-$GeSe_2$.

In view of the above findings, it is worthwhile to focus on the case of a perfect CON AX_2 network. Insightful information is provided by diffraction data on glassy GeO_2 [25] and by first-principles molecular dynamics results on liquid and amorphous SiO_2 [26, 27]. Due to the sizeable degree of ionicity in the bonding character, these systems are devoid of homopolar bonds and miscoordinations [26, 27]. As shown in figure 5, the FSDP is absent in the calculated $S_{CC}(k)$ partial structure factor of liquid and glassy SiO_2. These results are consistent with the absence of an FSDP in the measured $S_{CC}(k)$ of glassy GeO_2 [25].

5. Conclusions

We have shown that a change in composition from l-$GeSe_2$ to l-$GeSe_4$ has the effect of increasing the short-range chemical order and inducing the appearance of an FSDP in the calculated $S_{CC}(k)$ partial structure factor. Less effective is the increase of chemical order obtained by considering l-$SiSe_2$ instead of l-$GeSe_2$. In this case, only a small peak in the FSDP region becomes noticeable. Focusing on AX_2 disordered systems, it appears that fluctuations of concentration on intermediate-range distances do not occur in two situations representing

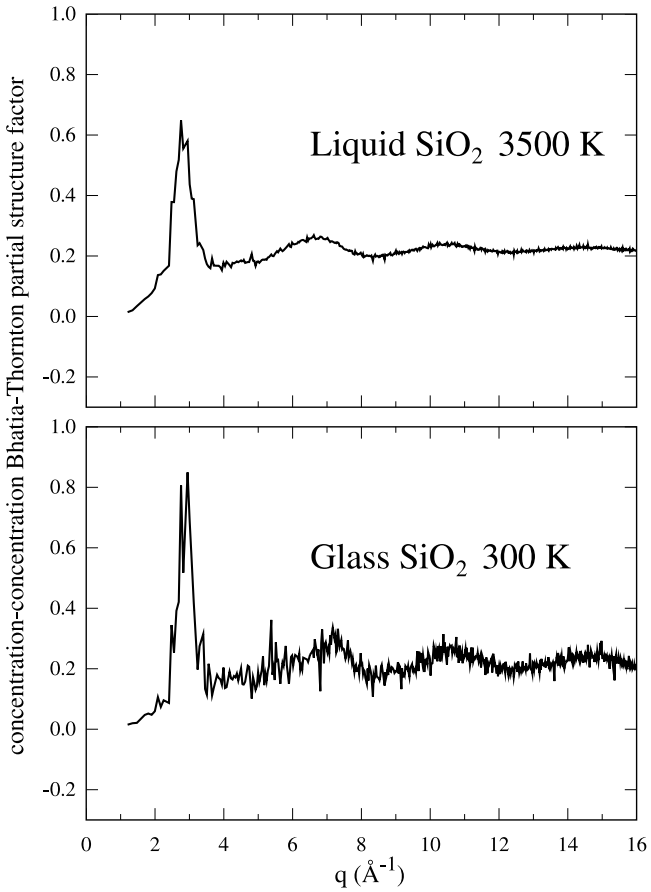

Figure 5. BT concentration–concentration partial structure factor $S_{CC}(k)$ for liquid SiO_2 and glassy SiO_2 (from the simulations described in [26] and [27]).

opposite structural topologies. The first situation corresponds to the absence of IRO and is due to the lack of a predominant short-range motif, as found in high-temperature l-$GeSe_2$ [28]. For this system, no FSDP is observed in any of the partial structure factors. The second situation corresponds to perfect chemical order, which leads to an FSDP in the total neutron structure factor but not to an FSDP in $S_{CC}(k)$. This is what happens in disordered SiO_2 and GeO_2. The experimental results for l-$GeSe_2$ prove that for intermediate conditions, characterized by chemical order coexisting with homopolar bonds, the FSDP can appear in the $S_{CC}(k)$ partial structure factor. While this behaviour is not reproduced at our level of theory, the present calculations yield an FSDP in the $S_{CC}(k)$ partial structure factor of l-$GeSe_4$, which is more chemically ordered than l-$GeSe_2$. This demonstrates that our approach is in principle able to account for the occurrence of fluctuations of concentration on intermediate-range distances. Moreover, it shows that the chemical order can be correlated to the occurrence of an FSDP in $S_{CC}(k)$. Given the intimate relationship between chemical order and the ionic character of bonding, it is conceivable that a more appropriate account of ionicity (i.e. a theoretical framework improving upon our present description of bonding) will eventually bring theory in full agreement with experiments, also for the case of l-$GeSe_2$.

References

[1] Salmon P S 1992 *Proc. R. Soc.* A **437** 591
[2] Elliott S R 1991 *Phys. Rev. Lett.* **67** 711
[3] Penfold I T and Salmon P S 1991 *Phys. Rev. Lett.* **67** 97
[4] Bhatia A and Thornton D 1970 *Phys. Rev.* B **2** 3004
[5] The explicit relationship between the three sets of partial structure factors commonly used, Faber–Ziman, Ashcroft–Langreth and Bhatia–Thornton [4], is given in
Waseda Y 1980 *The Structure of Non-Crystalline Materials* (New York: McGraw-Hill)
[6] Massobrio C, Pasquarello A and Car R 1998 *Phys. Rev. Lett.* **80** 2342
[7] Massobrio C, Pasquarello A and Car R 1999 *J. Am. Chem. Soc.* **121** 2943
[8] Massobrio C, Pasquarello A and Car R 2001 *Phys. Rev.* B **64** 144205
[9] Perdew J P, Chevary J A, Vosko S H, Jackson K A, Pederson M R, Singh D J and Fiolhais C 1992 *Phys. Rev.* B **46** 6671
[10] Perdew J P and Zunger A 1981 *Phys. Rev.* B **23** 5048
[11] Massobrio C, Pasquarello A and Car R 2000 *Comput. Mater. Sci.* **17** 115
[12] Haye M J, Massobrio C, Pasquarello A, De Vita A, De Leeuw S W and Car R 1998 *Phys. Rev.* B **58** R14661
[13] Boolchand P and Bresser W J 2000 *Phil. Mag.* B **80** 1757 and references quoted therein
[14] Celino M and Massobrio C 2002 *Comput. Mater. Sci.* **24** 28
[15] Ruska J and Thurn H 1976 *J. Non-Cryst. Solids* **22** 277
[16] Johnson R W, Price D L, Susman S, Arai M, Morrison T I and Shenoy G K 1986 *J. Non-Cryst. Solids* **83** 251
[17] Car R and Parrinello M 1985 *Phys. Rev. Lett.* **55** 2471
[18] Dal Corso A, Pasquarello A, Baldereschi A and Car R 1996 *Phys. Rev.* B **53** 1180
[19] Pasquarello A, Laasonen K, Car R, Lee C and Vanderbilt D 1992 *Phys. Rev. Lett.* **69** 1982
[20] Laasonen K, Pasquarello A, Car R, Lee C and Vanderbilt D 1993 *Phys. Rev.* B **47** 10142
[21] See Elliott S R 1990 *Physics of Amorphous Materials* (Essex: Longman)
[22] Maruyama K, Misawa M, Inui M, Takeda S, Kawakita Y and Tamaki S 1996 *J. Non-Cryst. Solids* **205–207** 106
[23] Petri I and Salmon P S 2002 *Physics and Chemistry of Glasses* **43c** 185
[24] Iyetomi H, Vashishta P and Kalia R K 1991 *Phys. Rev.* B **43** 1726
[25] Price D L, Saboungi M L and Barnes A C 1998 *Phys. Rev. Lett.* **81** 3207
[26] Sarnthein J, Pasquarello A and Car R 1995 *Phys. Rev. Lett.* **74** 4682
[27] Sarnthein J, Pasquarello A and Car R 1995 *Phys. Rev.* B **52** 12690
[28] Massobrio C, van Roon F H M, Pasquarello A and De Leeuw S W 2000 *J. Phys.: Condens. Matter* **12** L697